Research on flexible silver nanowire electrode for organic light-emitting devices

HU Jun-tao (胡俊涛)[1]*, **LI Jie** (李杰)[1,2], **ZHANG Geng-geng** (张庚庚)[1,2], **XU Kai** (许凯)[1], and **WANG Xiang-hua** (王向华)[1]

1. *National Engineering Lab of Special Display Technology, State Key Lab of Advanced Display Technology, Academy of Opto-Electronic Technology, Hefei University of Technology, Hefei 230009, China*
2. *School of Instrument Science and Opto-electronics Engineering, Hefei University of Technology, Hefei 230009, China*

(Received 13 January 2020; Revised 28 February 2020)

By spin-coating silver nanowires (AgNWs) and polymethyl methacrylate (PMMA), applying pressure imprint and plasma treatment, we obtained flat AgNW thin film with a sheet resistance of 20 Ω/sq and a transmittance of 78% at 550 nm with low surface roughness. No significant change in sheet resistance was observed after cyclic bending (bending radius is 5 mm) test and tape test. After 1 000 bending tests, the change rate of sheet resistance was only 8.3%. The organic light-emitting devices (OLEDs) were prepared by using such AgNW electrodes and a maximum brightness of 5 090 cd/m^2 was obtained. Compared with the AgNWs electrode without any treatment, the present AgNW electrodes have lower sheet resistance and better hole injection. Our results show spin-coated with flat layers, embossed and plasma-treated AgNW electrodes are suitable for manufacturing flexible organic optoelectronic devices.

Document code: A **Article ID:** 1673-1905(2021)02-0070-5

DOI https://doi.org/10.1007/s11801-021-0005-x

In recent years, display technology has profoundly affected people's lifestyles. With the increasing demand for display screens, it has become an important area of modern electronics research. Compared with traditional display, organic light-emitting devices (OLEDs) have higher brightness, higher color gamut, faster response time, and higher contrast. In addition, OLEDs have foldability characteristics, making them applicable to wearable devices and ultra-thin electronic display devices[1-8]. At present, the most widely used transparent electrode in OLED devices is indium tin oxide (ITO). However, due to the poor bendability of ITO and the scarcity of metal indium, ITO is not the best choice for flexible electrodes[9].

Currently, the electrodes used in the market to replace ITO are silver nanowires (AgNWs)[10,11], graphene[12,13], carbon nanotubes (CNT)[14], conductive ink[15], etc. Carbon nanotubes have high surface roughness due to high aspect ratio, graphene has a high sheet resistance, and conductive inks are also excluded due to low transmittance. AgNWs have been widely studied as ITO replacement electrodes due to their excellent transmittance and low sheet resistance. Nanowire thin films are often used in the production of devices based on the solution method. The methods for making AgNW electrodes are usually spin coating, screen printing, inkjet printing[16-18], etc. In these processes, the intersecting AgNWs are mainly attached to the PET substrate by gravity, which will cause the intersecting AgNWs to loosen and the adhesiveness between the intersecting AgNWs and the PET substrate to deteriorate, and generate a large sheet resistance. In order to reduce the sheet resistance and improve the adhesion between AgNW and the substrate, the commonly used methods are high temperature annealing, embossing, making composite electrodes, improving electrode manufacturing processes such as reverse peeling[19], etc.

In this study, we used a spin coating method and a suitable spin coating rate to deposite AgNWs on PET to produce a transparent anode that can be used in flexible OLEDs. Due to the higher aspect ratio of AgNWs, higher surface roughness results. And AgNW adhesion will become worse over time, which will affect the stability of device operation. In order to solve these problems, we use polymethyl methacrylate (PMMA) as a flat layer and apply a certain pressure, so that the surface roughness and sheet resistance of the AgNWs film are reduced and the adhesion is improved. Then plasma treatment is used to further reduce the surface roughness and sheet resistance of the AgNWs thin film so as to facilitate the

* E-mail: jthu@hfut.edu.cn

preparation of subsequent light emitting devices.

PMMA powder (purchased from Aldrich, M.W.: 996 000) was dissolved in water with anisole ($CH_3OC_6H_5$) to prepare a 4 wt% PMMA solution. AgNW suspension in water with 5 mg/mL was purchased from VIGON TECHNOLOGY, and the average diameter and length of the AgNWs were ~35 nm and ~25 μm. The procedure used for the fabrication of the AgNWs-based transparent electrode is schematically illustrated in Fig.1.

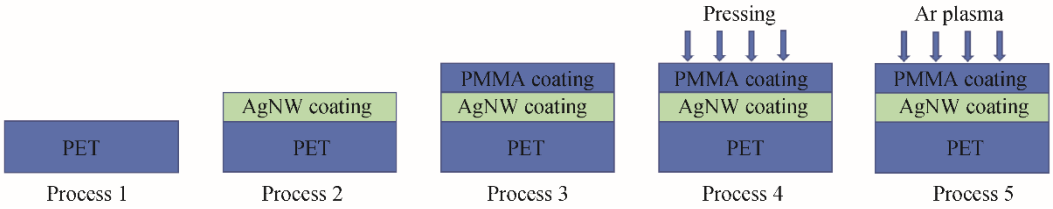

Fig.1 Procedure of the fabrication of the AgNWs-based transparent electrode

First clean the PET substrate with acetone, alcohol and deionized water in sequence. Then dry the water on the PET with nitrogen and heat the substrate at 100 °C for 10 min to dry to ensure that all the water is removed. On the cleaned PET substrate, first spin-coat AgNWs at a speed of 500 rpm/min for 5 s; then spin-coat AgNWs at a speed of 1 000 rpm/min for 25 s, then anneal at 140 °C for 10 min. As AgNW film has high surface roughness and poor surface adhesion, spin-coat PMMA on a substrate coated with AgNW at a rate of 1 000 rpm/min to reduce the surface roughness of the film and improve the adhesion of the film. The coating time was 60 s, followed by annealing at 100 °C for 10 min. In order to make the film surface evener, use a tablet press to apply 35 MPa pressure to embed AgNWs in PMMA. Plasma treatment (40 W) was performed on the AgNW film. To avoid the oxidation of the AgNWs, we choose Ar to generate the plasma.

OLEDs were fabricated using the treated AgNW as anode electrode. A 30-nm-thick MoO_3 was used as buffer layer, a 40-nm-thick NPB was used as the hole injection layer, a 60-nm-thick tris-(8-hydroxyquinoline) aluminum (Alq_3) was used as active layer and electron transport layer, and a 1-nm-thick LiF and 100-nm-thick Al film served as cathode.

In our work, thermal evaporation processed films were fabricated by a deposition chamber (Angstrom). Organic coating evaporation rate was 1 Å/s, the rate of evaporation for Al was 2 Å/s, and the rate of evaporation for LiF and MoO_3 were 0.5 Å/s. Transmittance spectra were recorded by UV 2550 ultraviolet spectrophotometer. The sheet resistance was measured with a four-probe ST-21 system. The surface roughness was measured using an atomic force microscope (AFM) (Dimension Icon, Bruker Corporation) in tapping mode. The current density-voltage (*J*-*V*) characteristics of the OLEDs were measured using a Keithley 2400 source measure unit (Tektronix).

We prepared three different electrodes. The processing process of device A is shown in steps 1 to 2 of Fig.1. The processing process of device B is shown in steps 1 to 4 of Fig.1. The processing process of device C is shown in steps 1 to 5 of Fig.1. Fig.2 shows atomic force microscopy (AFM) images of the surface of the electrodes for different processing processes. Fig.2(a) shows the root-mean-square surface roughness (R_{rms}) of the device A without any treatment. From the figure, the R_{rms} of the device A is 42.9 nm. Due to the high surface roughness in the figure, it is concluded that device A has more prominent nanowires. Such large surface fluctuations will lead to a higher possibility of device breakdown and electrical short circuit. It is obvious that surface roughness is clearly a property that affects the compatibility of transparent electrodes with the device. Fig.2(b) shows the AgNW thin film of device B which has been spin-coated with a flat layer and imprinted and the R_{rms} of 4.88 nm. By spin-coating ultra-thin layer of PMMA, the role of PMMA is to reduce the surface roughness of the AgNW film. We imprint AgNWs into PMMA to make the film more conductive. Fig.2(c) shows the AgNW thin film of device C after spin-on flat lamination and plasma treatment. Its R_{rms} is 4.60 nm. Compared with device A, device C also significantly reduces the surface roughness of the film.

At the same time, we measured the sheet resistance of device A with 50 Ω/sq using the four-probe ST-21 system, the sheet resistance of device B with 40 Ω/sq and the sheet resistance of device C with 20 Ω/sq. Plasma treatment can be used to reduce the sheet resistance of AgNW[20,21]. We believe that by controlling the plasma treatment time, AgNW can be melted and some non-conductive PMMA can be removed at the same time, which makes the AgNW sheet resistance lower. After comparative verification, the optimal plasma treatment time is 10 s in this experiment.

Fig.3 shows the optical transmittance characteristics of the electrodes. Electrodes A, B and C exhibited a high optical transmittance in the visible region,

which was not much different from the PET. Compared with device A, device B has a denser AgNWs stack by embossing, which fills more blank areas, thereby making the transmittance and sheet resistance lower than device A. Device C makes device performance better by using plasma processing. The effect of plasma on AgNWs can be manifested in two ways. First, the energy of the electrons in the low-temperature plasma at room temperature is very high, which can reach several electron volts. This energy is enough to destroy the covalent bonds in PVP and PMMA, so that they can be rapidly decomposed. And the plasma etching can quickly remove the PVP thin layer and PMMA flat layer on the AgNWs surface. The second is the thermal effect of the plasma. Due to the continuous collision of high-energy particles with AgNWs, part of the energy in the high-energy particles will remain on the AgNWs surface. With the accumulation of this part of the energy, the temperature of the AgNWs surface will gradually rise, eventually causing AgNWs surface melting phenomenon. After that, re-crystallization and fusion between adjacent AgNWs will occur, thereby reducing the contact resistance between AgNWs and improving the adhesion between AgNWs and the substrate[20,21].

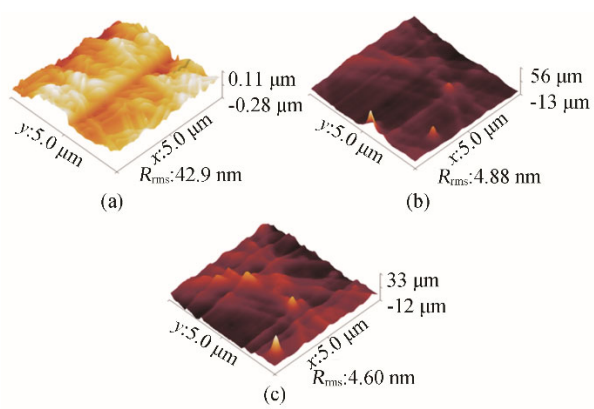

Fig.2 AFM topography images of (a) device A, (b) device B and (c) device C

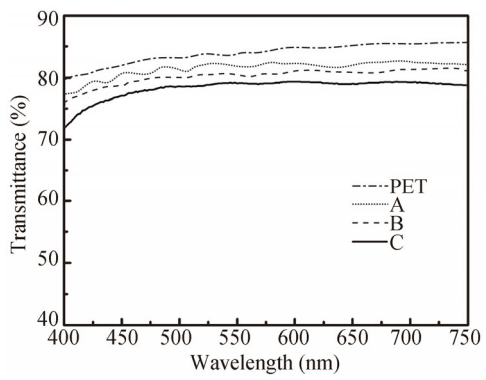

Fig.3 The transmittance curves of different electrodes

Fig.4 shows the change in sheet resistance during the bend and tape tests. Fig.4(a) shows the resistance change rate, obtained by a simple repeated bending of a film with a size of 44 mm×42 mm, curved surface of 44 mm and bending radius of 5 mm. Curves A, B, and C correspond to device A, device B, and device C, respectively. After 1 000 bending times, the resistance change rate of device A is the largest, and the resistance change rates of device B and device C are better than device A. Among them, the increase of the sheet resistance of the device C is less than 10% of the initial value, which is much lower than that of the device A and the device B. Fig.4(b) shows the change in sheet resistance of the device after repeated peeling with adhesive tape. A, B, and C in Fig.4(b) correspond to the resistance change curves of device A, device B, and device C, respectively. As can be seen from Fig.4(b), compared with the untreated device A, device B and device C have better adhesion. Due to the loose adhesiveness of AgNWs and PET substrate, AgNWs and PET substrate are easily separated. The AgNWs thin film of the device B added with the flat layer and the device C treated with the plasma layer were only slightly separated. This is because the added PMMA has stronger adhesion to PET after heating and the adhesion of AgNWs film is further strengthened after plasma treatment. Therefore, devices B and C processed by PMMA embossing and plasma have better mechanical stability and are expected to be suitable for applications of flexible optoelectronic devices.

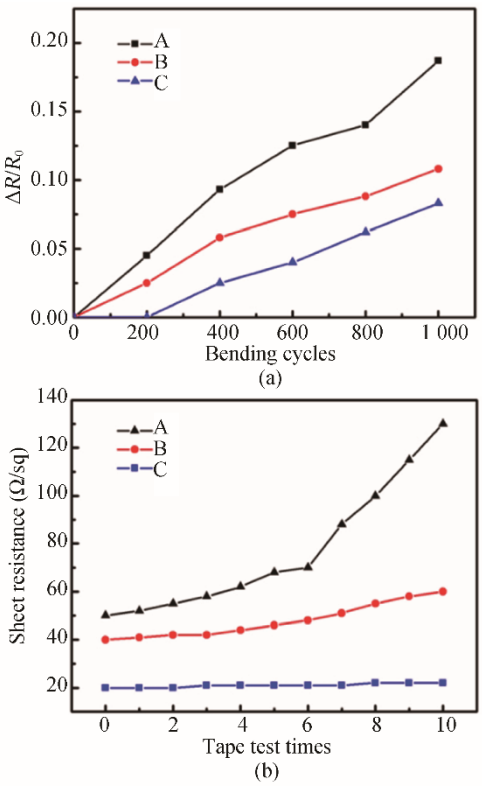

Fig.4 (a) Sheet resistance change rate during the test; (b) Sheet resistance change during the test

Fig.5 shows *L-V* and *I-V* characteristics of OLEDs prepared with AgNWs as anodes through different processing processes. Curve A in Fig.5 corresponds to device A, curve B corresponds to device B, and curve C corresponds to device C. We can see in Fig.5(a) that compared with the untreated device A, device B and device C show better optical characteristics. It can be seen from Fig.5(a) and (b) that the untreated device A has a breakdown at a lower voltage, resulting in a maximum brightness of only 258 cd/m^2, while the processed devices B and C have the maximum brightness. They are 2 414 cd/m^2 and 5 090 cd/m^2, which are much brighter than device A. Device B was spin-coated with a flat layer and embossed to obtain a flatter AgNW film. The spin-coated flat layer PMMA, embossing, and plasma-treated device C can provide good hole injection in the OLED, so that the device C has the best performance. After testing, the maximum brightness and current density of the OLED device prepared with device C as the anode were 5 090 cd/m^2 and 850 mA/cm^2, respectively. Compared with device A and device B, device C, which has been spin-coated with a flat layer, imprinted and plasma-treated, can improve the hole injection characteristics and make it very suitable for the manufacture of OLEDs.

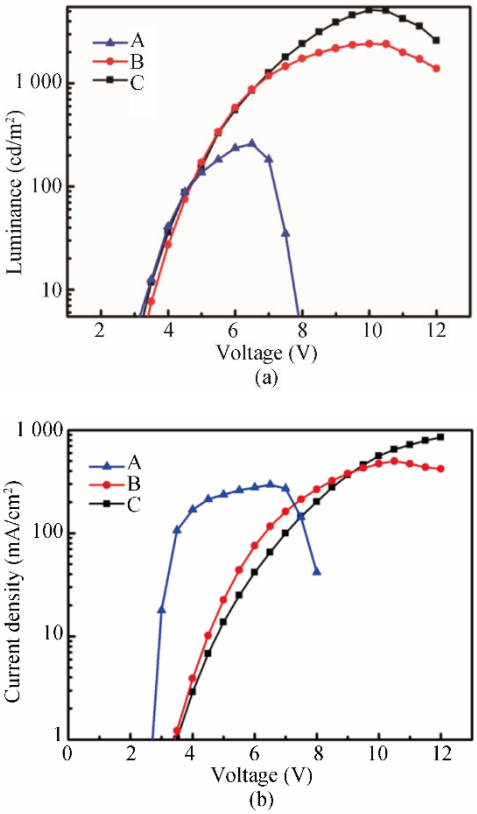

Fig.5 (a) luminance-voltage curves; (b) Current density-voltage curves

In summary, spin-coating PMMA flat layer, embossing and plasma treatment were conducted to prepare flexible AgNW electrodes. Spin coating PMMA, embossing can make the AgNW thin film more flat, while plasma treatment can greatly reduce the sheet resistance of AgNW, from 40 Ω/sq to 20 Ω/sq, while keeping the transmittance basically unchanged. This is because high-energy plasma can remove PVP and PMMA from the surface and fuse AgNWs together where AgNWs are in contact, thereby reducing the sheet resistance of AgNWs. Bent and tape tests were then performed on the spin-coated PMMA, embossed, and plasma-treated electrodes. Test results show that the electrode can maintain a low resistance change rate under 1 000 bending tests. In order to prove the applicability of this electrode in the construction of optoelectronic devices, we built an OLED device with AgNWs imprinted with spin-coated PMMA and plasma treated as the anode. Compared with the devices that have not undergone PMMA imprinting and plasma, the plasma-treated devices after spin-on PMMA imprinting exhibit better device performance. Our experiments show that the electrode properties of AgNW can be improved by spin-coating PMMA and embossing, followed by plasma treatment. The combined method of imprinting PMMA and plasma processing AgNWs can be applied to improve flexible photovoltaic devices in the future.

References

[1] Luo Y, Wang C, Wang L, Ding Y, Li L, Wei B and Zhang J, ACS Appl. Mater. Interfaces 6, 10213 (2014).

[2] Chen H W, Lee J H, Lin B Y, Chen S and Wu S T, Light Sci. Appl. **7**, 17168 (2018).

[3] Kim D H, Cho N S, Oh H Y, Yang J H, Jeon W S, Park J S, Suh M C and Kwon J H, Adv. Mater. **23**, 2721 (2011).

[4] Kim S, Kwon H J, Lee S, Shim H, Chun Y, Choi W, Kwack J, Han D, Song M, Kim S, Mohammadi S, Kee I and Lee S Y, Adv. Mater. **23**, 3511 (2011).

[5] Gaynor W, Hofmann S, Christoforo M G, Sachse C, Mehra S, Salleo A, McGehee M D, Gather M C, Lussem B, Muller-Meskamp L, Peumans P and Leo K, Adv. Mater. **25**, 4006 (2013).

[6] Meng H, Luo J, Wang W, Shi Z, Niu Q, Dai L and Qin G, Advanced Functional Materials **23**, 3324 (2013).

[7] Yun S O, Hwang Y, Park J, Jeong Y, Kim S H, Noh B I, Jung H S, Jang H S, Hyun Y, Choa S H and Ko H C, Adv. Mater. **25**, 5626 (2013).

[8] White M S, Kaltenbrunner M, Głowacki E D, Gutnichenko K, Kettlgruber G, Graz I, Aazou S, Ulbricht C, Egbe D A M, Miron M C, Major Z, Scharber M C, Sekitani T, Someya T, Bauer S and Sariciftci N S, Nature Photonics **7**, 811 (2013).

[9] Paine D C, Whitson T, Janiac D, Beresford R, Yang C O and Lewis B, Journal of Applied Physics **85**, 8445 (1999).

[10] Fievet F, Lagier J P and Figlarz M, MRS BULLETIN **14**, 29 (1989).
[11] Sun Y, Yin Y, Brian T M, Herricks T and Xia Y, Chem. Mater. **11**, 4736 (2002).
[12] Kwon K C, Kim S, Kim C, Lee J L and Kim S Y, Organic Electronics **15**, 3154 (2014).
[13] Yang G, Lee C, Kim J, Ren F and Pearton S J, Phys. Chem. Chem. Phys. **15**, 1798 (2013).
[14] Liu J, Li Y, Wang S, Ling Z, Lian H, Xu T, Zhang X, Liao Y and Wei B, Journal of Alloys and Compounds **814**, 152299 (2020).
[15] Li D, Lai W Y, Zhang Y Z and Huang W, Adv. Mater. **30**, 1704738 (2018).
[16] Friend R H, Gymer R W, Holmes A B, Burroughes J H, Marks R N and Taliani C, Nature **397**, 121 (1999).
[17] Zheng H, Zheng Y, Liu N, Ai N, Wang Q, Wu S, Zhou J, Hu D, Yu S, Han S, Xu W, Luo C, Meng Y, Jiang Z, Chen Y, Li D, Huang F, Wang J, Peng J and Cao Y, Nat. Commun. **4**, 1971 (2013).
[18] Pardo D A, Jabbour G E and Peyghambarian N, Adv. Mater. **12**, 1249 (2000).
[19] Nam S, Song M, Kim D H, Cho B, Lee H M, Kwon J D, Park S G, Nam K S, Jeong Y, Kwon S H, Park Y C, Jin S H, Kang J W, Jo S and Kim C S, Sci. Rep. **4**, 4788 (2014).
[20] Liston E M, Martinu L and Wertheimer M R, Journal of Adhesion Science and Technology **7**, 1091 (1993).
[21] Liston E M, The Journal of Adhesion **30**, 199 (1989).